

---

# Optimized Active Contour-Based Segmentation and Deep Belief Network For Brain Tumor Classification

(IJGASR) International Journal For  
Global Academic & Scientific Research  
ISSN Number: 2583-3081  
Volume 5, Issue No. 2, 80–108  
©The Author(s) 2026  
journals.icapsr.com/index.php/ijgasr  
DOI: 10.55938/ijgasr.v5i2.346

**IJGASR**

Jayaraj Ramasamy<sup>1</sup>, Srinath Doss<sup>2</sup>, Ashish Khanna<sup>3</sup>, Bal Virdee<sup>4</sup>

## Abstract

Magnetic Resonance Imaging (MRI) is widely used for detecting abnormal brain tissues; however, accurate tumor identification and classification remain challenging due to image variability and noise. This study proposes an efficient framework for automated brain tumor detection and classification. Initially, MRI images undergo preprocessing, including denoising and skull stripping, to enhance image quality. Tumor segmentation is performed using an optimized active contour model with a tuned weighting factor for precise boundary extraction. Discrete Wavelet Transform (DWT)-based features are then extracted to capture discriminative spatial–frequency information. These features are classified using an Optimized Deep Belief Network (DBN), where network weights are fine-tuned using the Improved Bat Algorithm (BA). Compared to conventional optimizers, the BA-based optimization provides faster convergence, better global search capability, and reduced risk of local minima, leading to improved classification performance. The proposed model is evaluated on a benchmark dataset using metrics such as accuracy, precision, sensitivity, and specificity. Experimental results demonstrate that the proposed approach achieves superior performance and robustness compared to existing methods for brain tumor detection.

## Keywords

Brain Tumor Classification, Optimized Active Contour, Discrete Wavelet Transform, Deep Belief Network, Bat Algorithm

**Received:** 24 December 2025; **Revised 1:** 24 April 2026; **Revised 2:** 22 May 2026;  
**Accepted:** 29 May 2026; **Published:** 02 June 2026;

---

<sup>1</sup>Department of Computing, De Montfort University, Kazakhstan. Center for Communications Technology, London Metropolitan University, London, U.K.

<sup>2</sup>Faculty of Engineering and Technology, Botho University, Botswana. Center for Communications Technology, London Metropolitan University, London, U.K.

<sup>3</sup>Department of Computer Science and Engineering, Maharaja Agrasen Institute of Technology (GGSIPTU), Rohini, India

<sup>4</sup>Centre for Communications Technology, London Metropolitan University, London, U.K.

## Corresponding author:

Email: jayarajrcse@gmail.com



## Introduction

According to a National Cancer Society USA (NCSUS) report<sup>[1]</sup>, brain tumours have been found in 6.8 million people. An abnormal growth of cancerous or non-cancerous brain cells which may be benign or malignant is known as a brain tumor. In addition to having a non-uniform appearance, malignant cells vary from benign lesions in that they include living cancer cells. Benign tumors are uniformly shaped and lack living cell<sup>[2]</sup>. Primary and metastatic tumors make up both categories. As opposed to malignant tumours, which are made up of cancerous cells that have spread from the affected area of the body into the brain, primary brain tumors are still mostly made up of brain cells. Amongst some of the challenges in identifying brain lesions from MRI (Magnetic Resonance Imaging) images are segmentation, tumor detection, and categorization. Deep learning methods have great promise for improving the precision and consistency of brain tumor diagnosis. To diagnose brain tumors, computer-aided methods are primarily used to gather significant clinical data on the incidence, localization, and kind of the tumor<sup>[3]</sup>. The detection of tumors has grown to be challenging due to the brain's intricate anatomy. For more effective illness management, early tumor diagnosis and disease progression estimation are essential. Because the cancer range in the brain image must now be established manually in clinical applications, manual processing becomes impractical for vast amounts of data. Practical work and cancer treatment are significantly impacted by the detection of malignancies utilizing abnormal Magnetic Resonance Images (MRI). One of the hardest medical specialties is the imaging of brain tumors using MRI technology. High-quality images of human body components can be produced using advanced medical imaging equipment known as MRI. Radiologists should be able to accurately diagnose tumors, but this takes time. Experience has shown that tumor diagnosis can be accomplished using machine imaging and image synthesis. The development of new imaging techniques helps physicians monitor and track the progression of tumor growth at varying phases. Software-based MRI image processing for more precise detection benefits greatly from the classification of MRI brain image information. The classification method is obviously made more difficult by the noise and artefacts that can significantly affect MRI images due to the shortcomings of image-gathering systems<sup>[4]</sup>. Brain anatomy can be accurately determined by MRI, although segmentation of medical data might be difficult due to issues like poor positioning accuracy, weak contrast, inhomogeneity, and unsteady object form<sup>[5]</sup>. Recognition is made more difficult by the radio-frequency coil's non-uniformity and the image's blurred morphology of the tissues' borders<sup>[6]</sup>. The threshold-based, geographical area, designer, and Artificial Neural Network (ANN) approaches are computer-supported techniques for classifying medical images. Because of their outstanding classifier performance, Convolutional Neural Networks (CNN), a deep learning technology, have recently been found to be very beneficial in the categorization of medical images<sup>[7]</sup>. A neural network with several hidden units and free features is called a convolutional multi-layer and does deep learning. The convolution layer, a pooling layer, filters/kernels, fully-connected levels, and components for the ultimate decision-making process are all managed by this application for each incoming MRI image<sup>[8]</sup>.

By utilizing one of the CNN approaches, our research aims to offer an Optimized active contour methodology for segmentation technique on MRI brain images. Additionally, CNN will be used in order to diagnose tumors as accurately as feasible. The data collection was from the BRATS imaging information, which consists of brain scans performed using four different MRI techniques. Following is a summary of the suggested paper's research contributors:

- A brand-new automated technique for detecting brain tumors is suggested.
- An optimized active contour approach is adopted for segmenting the tumor.
- For feature extraction, Discrete wavelet features are used.
- For classification, a Deep Belief Network (DBN) is used.
- The proposed algorithm optimises the DBN using Bat Algorithm.

The novelty of the proposed framework lies in the integration of optimized active contour-based segmentation, DWT feature extraction, and Deep Belief Network (DBN) classification enhanced through the Improved BA within a unified pipeline for brain tumor analysis. Unlike conventional approaches that rely only on deep learning architectures, the proposed model combines spatial-frequency feature representation with optimization-driven learning to improve classification stability and accuracy while maintaining reduced computational complexity. The optimized active contour model enables precise tumor boundary localization, whereas DWT efficiently captures discriminative texture and frequency-domain information from MRI images. Furthermore, the Improved Bat Algorithm enhances DBN weight optimization by accelerating convergence and avoiding local minima during training. The framework can assist radiologists in reducing manual interpretation burden, improving diagnostic consistency, and enabling early tumor detection. In addition, the modular structure of the proposed method allows adaptability to different MRI datasets and healthcare environments, thereby increasing its applicability for practical medical image analysis tasks.

**Organization of paper:** Since we already came across the introductory part in Section 1, the remaining sections are arranged as: Section 2 demonstrates similar works, Section 3 portrays methodology, Section 4 illustrates the performance Analysis of the segmentation approach, and finally, Section 5 ends the paper with a conclusion.

## Literature Survey

Among the most crucial techniques for analyzing clinical data is image classification, which offers details about serious illnesses like brain tumors. Despite numerous studies on braintumour segmentation, extracting a precise tumour structure remains a difficult task.

This section explores different works that deal with brain tumour segmentation and classification using optimization-based schemes. A strategy to lessen the complexity of the system was put up by Bahadure et al.<sup>[9]</sup>. The brain tumor's determination was made using the Berkeley Wavelet Transformation. Additionally, to increase system performance, specific characteristics were included that are retrieved from the images and injected into an SVM to classify them. Overall, the results were 97% accurate, 98% sensitive, and 94% accurate.

<sup>[10]</sup> created a k-means clustering approach and mathematical morphology-based brain tumor diagnosis MRI image sensor. The technique eliminates the possibility of erroneous areas being created after segmenting the brain MRI image. Bauer et al.<sup>[11]</sup> also showed an efficient algorithm for fragmenting brain cells that combines SVM with textures, multitemporal intensities, and conditional random fields. The suggested approach showed quick and dependable results. To reduce complexity and increase system efficiency, Shree et al.<sup>[12]</sup> developed a thorough strategy that included noise removal, feature

extraction, and DWT-based segmentation. After categorization, the noise was reduced using mathematics morphogenesis. The area of the tumour was subsequently classified using the backpropagation algorithm. The categorization accuracy of the experimental data was nearly 100%.

An excellent method utilizing artificial neural networks and k-means was described by<sup>[13]</sup>. To diagnose the cancer cells, a fuzzy controller was also developed using the characteristics that were gathered. The method was utilized to determine the tumor's location and size from an MR image. For the classification of images of brain tumors into four groups,<sup>[14]</sup> used Deep Neural Network (DNN) classifiers. The network used DWT's retrieved characteristics with exploratory factor analysis-based pruning. The great reliability of the performance and efficiency was demonstrated by experimental data. For the extraction of the MR brain images,<sup>[15]</sup> suggested using kernel sparse coding and texture features.

Joseph et al.<sup>[12]</sup> showed brain tumor detection with segmentation in MRI. Image processing is a challenging field in which active research work is going on. Utilizing diagnostic imaging methods, the body's internal organs were found. A brain tumor is a dangerous condition that can change a person's life. When the medical images were processed, the segmentation played a vital role in detecting suspicious areas.

M.A. Ganaie et al.<sup>[16]</sup> showed the segmentation fusion using MRI to detect brain tumors. Magnetic Resonance Images (MRI) consumed more time and tended to be error-prone while segmenting the brain tumor manually. A novel algorithm was implemented to acquire a fused segmentation with the use of other methods and it was termed Potential Field Segmentation (PFS). A new strategy for classifying broadly that takes into account their commonality across physics is called artificial potential splitting. An MRI scan that produced a projection matrix showed the device's brightness as a bulk. The potential field was calculated exactly for all the pixels in MRI. Afterwards, if the computation was fewer than the adaptive potential threshold, the tumor region was identified with its associated pixel. This segmentation criterion was found to be instinctively effective because of a greater mass of tumor pixels. Finally, the neighbourhood region had more potential when compared to other regions containing lesser mass or no mass. Recent advances in brain tumor segmentation and classification have increasingly focused on attention-based deep learning models, Vision Transformers (ViT), hybrid CNN-transformer architectures, and advanced U-Net variants to improve feature representation and localization accuracy. Transformer-based architectures have demonstrated strong capability in capturing long-range contextual dependencies through self-attention mechanisms, thereby improving segmentation robustness in heterogeneous MRI datasets. Swin UNETR incorporated hierarchical Swin Transformer blocks to U-net and performed well on both multimodal brain tumor segmentation problems, enabling the network to capture long-range spatial interactions<sup>[17]</sup>. Likewise, TransBTS used transformer encoder in conjunction with CNN-based architectures to enhance the volumetric feature extraction and global contextual learning for MRI brain tumor segmentation<sup>[18]</sup>. Hybrid transformer-U-Net architectures have also attracted a lot of interest in recent years. BiTr-Unet incorporated CNN feature extraction and transformer-based contextual modeling to enhance the boundary localization and consistency of tumor segmentation<sup>[19]</sup>. To enhance the performance of semantic feature fusion and spatial recovery, U-Transformer added self-attention and cross-attention modules into the U-Net network<sup>[20]</sup>. There are also several recent studies investigating attention enhanced U-net models for increased segmentation accuracy. Optimized U-Net architectures with residual learning, deep supervision, focal loss and decoder attention mechanism showed good results in BraTS benchmark datasets<sup>[21]</sup>. To further enhance tumor localization and feature discrimination in challenging MRI settings, attention-based multi-scale U-Net models and EfficientNet-based U-Net

frameworks were also presented. Transferred Vision Transformers (ViTs) have been shown to be effective for brain tumor diagnosis for multiple classes directly from MRI patches<sup>[22]</sup>. Moreover, transformer attention was combined with multi-task learning as adaptive transformer frameworks like BrainTumNet, which jointly achieved segmentation and classification tasks with better diagnostic performance<sup>[23]</sup>. Recently, there have been also some attempts to perform simultaneous segmentation and classification by means of generative transformer-based approaches. The BT-GANformer generative transformer model that was developed by the author's team enabled high-accuracy analysis of multimodal MRI using CNN and transformer modules and achieved better Dice similarity and ROC-AUC results<sup>[24]</sup>. Ensemble of transformer based segmentation models further enhanced the feature aggregation and contextual representation learning without sacrificing computational efficiency<sup>[25]</sup>. Despite these developments there are still a number of widely used deep learning models based on transformers and hybrid models that suffer from high computational complexity, high memory consumption, and a significant reliance on large amounts of training data. The large volume of annotated data and significant amount of GPU power are also needed in many architectures in order to be convergent. Thus, it is still desirable to find frameworks that are optimization-oriented, computation efficient, and can retain competitive segmentation and classification performance at moderate size datasets and low computational cost. While there are a number of existing studies that have shown encouraging performance in brain tumor segmentation and classification, there are still a number of challenges in terms of computational speed, feature representation, robustness and generalization. Most traditional ML methods are based on hand-crafted features (SVM, k-means clustering and fuzzy-based methods) and lack adaptability with complex MRI variations and complex tumor structures. Furthermore, most of these methods need a lot of tuning and pre-processing to ensure consistent performance. In recent years, the automatic feature learning and classification accuracy have been enhanced by deep learning based models such as CNN and DNN architectures. Deep CNN models, however, typically require large amounts of annotated data and compute power, and may limit their ability to be used in clinical settings where data is limited. Moreover, most of the existing studies tend to concentrate only on classification accuracy and offer a brief discussion on computational complexity, runtime efficiency, statistical validation and model interpretability. In recent years, transformer-based architectures have also been the focus of interest for their self-attention capabilities to model long-range dependencies. While they are effective, they tend to be memory-intensive, complex in parameters and require more training time. Transformer models could be prone to overfitting and computational complexity issues in specific medical imaging tasks where datasets are moderate in size. Moreover, a vast number of previous studies separately implement segmentation and classification without taking into account the effect of optimization applied to the preprocessing, correct placement of the tumor, discriminative feature extraction, and optimization based classification in a single system. Others are not well validated by cross validation techniques and statistical significance testing and so the claimed performance gains are less trustworthy. To overcome these drawbacks, the proposed scheme combines the optimized active contour segmentation, DWT-based feature extraction, and classification using Improved Bat Algorithm based DBN in a single scheme. The overall goal of the framework is to achieve a compromise between accuracy of classification, computational efficiency, robustness and feasibility for clinical applications in real world.

## Methodology

A brain tumor is a more lethal condition that causes more deaths than survivors. Automated computer-based brain tumor image processing is getting more and more popular in the modern day as a result of the development of technologies. Tumor segments and tumor identification are the two most significant tasks that have been discussed for the investigation of brain tumors. Although several classification algorithms were introduced by the researchers, still there exist some problems in classification accuracy that needs to be improved. By doing so, this idea aims to create a brand-new brain tumor categorization model. Fig. 1 displays the suggested categorizing paradigm for brain tumors. Initially, pre-processing is performed which involves steps like, denoising and skull stripping. Subsequently, segmentation takes place via an Optimized active contour approach, where, the weighting factor will be optimally tuned. Further, feature extraction is carried out, where DWT based features are extracted. These features will be then classified using an Optimized DBN, where the weights will be optimally chosen employing an improved algorithm. Here we use the Modified BA, a global metaheuristic optimization algorithm, for improvement. It was modelled after the variable pulsing speeds and intensity of echolocation used by microbats. A detailed explanation is given in the below sections.

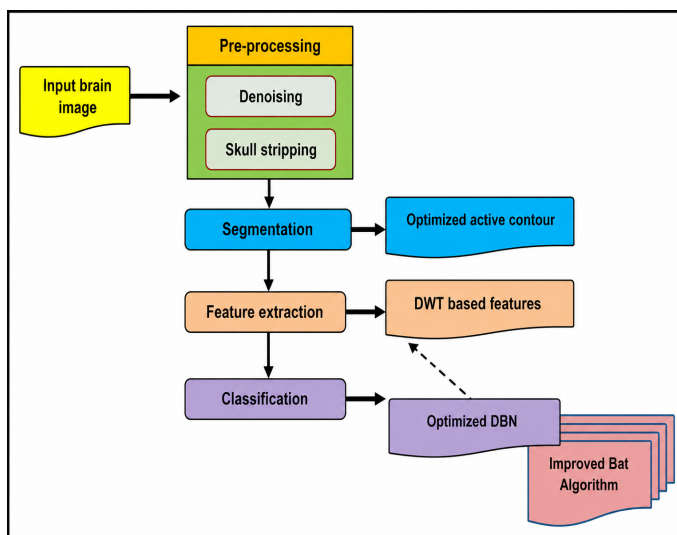


**Figure 1.** Block diagram of Proposed Brain Tumor Classification model (AI Generated)

### Preprocessing

To begin with, preprocessing is conducted in order to optimize the quality of MRI images and guarantee the quality of the analysis of tumors. This step includes denoising, skull stripping, normalization and data preparation.

Whole brain segmentation, also known as skull stripping is done to eliminate non-cerebral tissue, which includes the skull, fat tissue, muscle, and the connective tissue<sup>[26]</sup>. This step centers the analysis

on the parts of the brain and enhances better segmentation. To effectively extract brain tissues in multi-sequence MR images, a hybrid method made of thresholding and morphological operations are used.

After this intensity normalization is used to standardize pixel values to a range between 0 and 1, so that all samples have equal values and convergence of model is faster. Data augmentation methods like rotation, flipping, and scaling are used to further improve the generalization of the model and minimize overfitting.

The processed data is further divided into training, validation and testing sets in the proportion of 70:15:15 and the class distribution is balanced.

### Segmentation

Active Contour model is a technique used for segmentation, which has been introduced by Kasetal<sup>[27]</sup>. The outcome of segmentation in the Active Contour model relies on the initial contour. The initial Contour  $IR(x, y)$  in the Active Contour model shifts to the tumor boundary. The total energy of the snake can be calculated using the expression,

$$E_{tot} = \int_i^1 E_s (v(s)) ds \quad (1)$$

Where  $v(s)$  is the parametric representation of the curve, given by:

$$v(s) = [x(s), y(s)] \quad (2)$$

$E_s$  is the internal energy and  $ds$  is the external energy of the snake. These internal and external energies are the two components of total energy  $E_{tot}$ . **Optimized Active Contour Parameter Tuning**  
In the proposed segmentation framework, the weighting parameter controlling the balance between internal contour smoothness and external image-driven forces was optimized to improve tumor boundary localization accuracy. The optimization process was performed using the Improved Bat Algorithm (BA), which adaptively searches for the optimal weighting factor that minimizes segmentation error. The active contour energy function consists of internal energy and external energy terms and is expressed as follows in Equation (3).

$$E_{total} = \alpha E_{(internal)} + \beta E_{external} \quad (3)$$

where  $\alpha$  controls contour smoothness and  $\beta$  controls attraction toward tumor boundaries. In this study, the weighting parameter  $\beta$  was optimized to achieve accurate contour evolution and reduced boundary leakage during segmentation.

The optimization objective was defined to minimize segmentation error between the segmented tumor region and the corresponding ground truth annotation. The objective function was formulated using Dice loss as follows in Equation (4):

$$\text{Loss} = 1 - \frac{2|S \cap G|}{|S| + |G|} \quad (4)$$

where  $S$  represents the segmented tumor region and  $G$  denotes the ground truth region.

During optimization, the Improved Bat Algorithm iteratively updated the weighting parameter using population-based search and adaptive frequency tuning. After multiple experimental evaluations, the

optimal weighting parameters were determined as  $\alpha = 0.4$  and  $\beta = 0.6$ , which provided the best balance between contour smoothness and tumor boundary adherence. The optimized active contour model significantly improved segmentation accuracy by reducing over-segmentation and background interference while preserving fine tumor boundaries.

### Feature Extraction

Colour, pixel intensity, texture, and shapes are the main features of MRI scan images considered for feature extraction. Here, the DWT (Discrete Wavelet Transform)<sup>[28]</sup> method is used for feature extraction. The computed wavelet coefficients confine the frequency data of signals, which are important factors in tumour categorization.

Based on its resolution concerning the frequency scale, the various frequency components are as follows:

$$F_{DWT}(s) = \left\{ EA_{i,j} = \sum_0^1 f(s) h(s) * i(s - 2ij), \quad EA_{i,j} = \sum_0^1 f(s) l(s) * i(s - 2ij) \right\} \quad (5)$$

### Classification

The Deep Belief Network (DBN), with the weights improved by the given Bat Algorithm (BA), classifies the brain cancer images into regular and pathological in the crucial stage. The DBN was chosen over other modern architectures that are more computationally intensive due to its ability to provide stable performance classification results with relatively small training complexity and low data dependency. The recent transformer based and very deep CNN architectures have good performance, but they need very large annotated datasets, lots of computing resources and longer training time for optimal generalization. For moderate-sized medical imaging datasets, however, DBN is well suited and can effectively learn hierarchical representations of features with fewer training parameters. In the proposed framework, the extracted features from MRI images based on DWT are used to minimize the feature redundancy before classification stage. Thus, the complex nonlinear relationships can be sufficiently learned by a DBN classifier without the need of excessively deep architectures. In addition, the Improved BA is used to optimize network weights, speed up convergence and lessen the chances of local minima during the training phase of the DBN. The computational efficiency and practical clinical usability are another crucial factor in the choice of DBN. In contrast to transformer-based models, DBN also uses less memory and has lower inference speed, which is particularly suitable for practical applications in medical fields such as real-time processing or resource-limited settings. In comparison with transformer-based approaches, DBN could be more feasible for real-time or resource-constrained medical settings with lower memory usage and inference time. The proposed DBN-based framework is also found to be competitive in terms of accuracy compared to recent CNN and transformer models through experimental comparisons, with lower computational complexity and better optimization efficiency. The structure that deep learning uses, which is built on automatically extracting features using low-level sources, is its main advantage. During this, DBN contains a range of hidden layers with Boltzmann machines restricted as the fundamental units<sup>[29]</sup> initially described this system. Every layer of the DBNs has a Restricted Boltzmann Machine (RBM), which is learned through supervisor learning. This phase includes developing the networks and reducing over-fitting by searching the weights area.

Remembering that just over happens whenever the training rates are very low and the testing mistake is crucial. To enhance its capacity to discriminate amongst categories, DBN can extract particular aspects from the learning algorithm. The basic design of the RBM is shown in Figure 2. In Figure 2, the letters  $v$  and  $h$  stand in for the viewable layer and the invisible layers, respectively. The model is instructed to move the pieces hidden from view at  $h$ ,  $\in [0, 1]$ .

Biases and unfocused weights ( $w_{ij}$ ) have been assumed to exist between any of these layers in contrast to accessible and hidden layers. The probabilistic model of the revealed and hidden layers is defined by the functional form, as illustrated in Calculations (4).

$$p(v, h) = \frac{1}{\sum_{v,h} e^{-E(v,h)}} e^{-E(v,h)} \quad (6)$$

wherein  $E(v, h)$  denotes the RBM's energy function and is expressed as Equation (5):

$$E(v, h) = - \sum_{i=1}^n a_i v_i - \sum_{j=1}^n b_j h_j - \sum_{i,j} v_i h_j w_{ij} \quad (7)$$

wherein  $w_{ij}$  denotes the weight between the hidden and visible layers, and  $a_i$  and  $b_j$  are the bias parameters for the visible and hidden units, respectively. In Equation (6), the probability of a system is calculated.

$$P(v, h) = \frac{e^{-E(v,h)}}{\sum_{v,h} e^{-E(v,h)}} \quad (8)$$

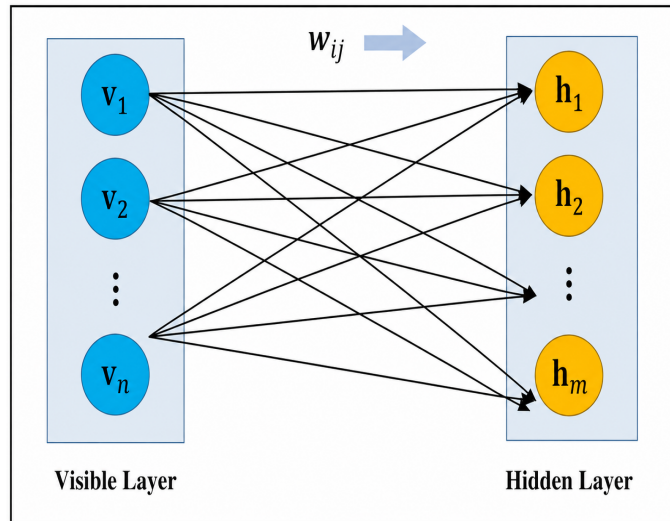


**Figure 2.** Graphical representation of the RBM architecture used within the DBN

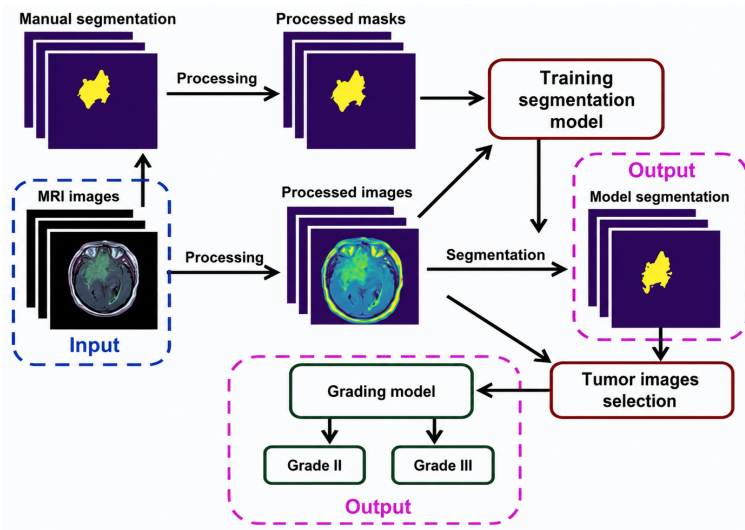


**Figure 3.** Proposed classification pipeline integrating preprocessing, optimized segmentation, DWT feature extraction, Improved Bat Algorithm optimization, and DBN classification

Figure 3 separately presents the complete proposed classification framework, including preprocessing, optimized active contour-based segmentation, DWT feature extraction, Improved Bat Algorithm-based optimization, and final DBN classification stages. A brand-new swarm intelligence technique called the bat algorithms was put forth by [30]. The way that bats use echolocation to gauge altitudes is an inspiration for this optimization approach. Bats emit a loud sound pulse and listen for the echo that emanates from items. To find prey, bats fly at diverse angles and at varying speeds. Regardless of the type of bat, their pulses have different characteristics. Mimicking how bats find their meal, the bat algorithm was developed. In the bat algorithm, each bat symbolizes a population-level answer.

The frequency, velocity and position of each bat are thus updated in the population for subsequent movements. This is because the bat algorithm makes use of the frequency tuning process to ensure diversity among solutions within the population. One of the benefits of using this algorithm is that it allows for the fusion of population-based algorithms with local searches. The role of the pulse rate and loudness is to control the balance between population-based and local searches. The bat algorithm makes use of the variations in pulse rates and loudness of bats to ensure an effective balance between exploration and exploitation in the process of searching. There are several simplifications and idealizations concerning bat behaviour that have been considered and introduced in this algorithm by Yang [30]. This algorithm operates according to a process whereby a collection of solutions is altered through a random signal bandwidth increase, using harmonics. This change occurs in subsequent iterations, and loudness and pulse rates of solutions are updated after each iteration. Frequency, velocity and position of solutions are obtained from the below equations.

$$f_i = f_{min} + (f_{max} - f_{min})\beta \quad (9)$$

$$v_i^t = v_i^{(t-1)} + (x_i^{(t-1)} - x_{gbest}^t) f_i \quad (10)$$

$$x_i^t = x_i^{t-1} + v_i^t \quad (11)$$

The  $\beta$  is a number between  $[0, 1]$ ,  $f_i$  is the  $i^{th}$  bat's frequency, which determines the area and velocity of its movements,  $v_i$  and  $x_i$  are its velocity and location, respectively, and  $x_i^{gbest}$  is the overall best solution at time step  $t$ .

This strategy evaluates the use of such benefits of search engines in order to maintain the range of answers provided by the community. A strategy that helps was taken into consideration while the algorithms employed the selection method for the alternatives. The random walk approach is used in this search strategy to produce a fresh answer.

### Improved BA

The standard BA provides efficient global optimization through echolocation-inspired position and velocity updates. However, the conventional BA may suffer from premature convergence and reduced local search efficiency during later optimization stages. To overcome these limitations, an Improved Bat Algorithm (IBA) was introduced in this study by incorporating adaptive loudness updating and dynamic inertia-based velocity control.

In the conventional BA, the velocity update is expressed as follows in Equation (10):

$$v_i^t = v_i^{t-1} + (x_i^{t-1} - x_{best})f_i \quad (12)$$

and the position update is given by Equation (11):

$$x_i^t = x_i^{t-1} + v_i^t \quad (13)$$

where  $x_i^t$  and  $v_i^t$  represent the position and velocity of the  $i^{th}$  bat at iteration  $t$ ,  $x_{best}$  denotes the current global best solution, and  $f_i$  is the pulse frequency.

In the proposed Improved Bat Algorithm, an adaptive inertia weight term was introduced into the velocity update equation to improve exploration during early iterations and exploitation during later iterations. The modified velocity update rule is defined as follows in Equation (12):

$$v_i^t = \omega v_i^{t-1} + (x_i^{t-1} - x_{best})f_i \quad (14)$$

where the adaptive inertia weight  $\omega$  is computed as follows in Equation (13):

$$\omega = \omega_{max} - \left( \frac{\omega_{max} - \omega_{min}}{T} \right) t \quad (15)$$

Here,  $\omega_{max}$  and  $\omega_{min}$  denote the maximum and minimum inertia weights,  $t$  is the current iteration number, and  $T$  is the maximum number of iterations.

Additionally, the loudness and pulse emission rates were adaptively updated to balance global and local search processes in Equation (14) and Equation (15).

$$A_i^{t+1} = \alpha A_i^t \quad (16)$$

$$r_i^{t+1} = r_i^0 [1 - \exp(-\gamma t)] \quad (17)$$

where  $A_i$  represents loudness,  $r_i$  denotes pulse rate, and  $\alpha$  and  $\gamma$  are adaptive control parameters.

The proposed modifications improve convergence stability, enhance global search capability, and reduce the probability of trapping in local minima during DBN weight optimization. Experimental observations demonstrated improved optimization performance and enhanced classification accuracy using the proposed Improved Bat Algorithm. that the Improved Bat Algorithm achieved faster convergence and higher classification accuracy compared to the standard BA. The combination of various elements of the proposed framework is based on the necessity to overcome the complexity of challenges that can be posed by the identification of brain tumor on the MRI images. The parts are all designed to do a specific and complementary job, making sure of a better overall performance. The preprocessing phase, which involves denoising and skull stripping, improves the quality of the image by eliminating noise and other non-relevant non-brain tissues, thus, improving the credibility of the further process. The active contour-based segmentation is optimized to achieve a fine localization of the tumor which minimizes the background interference and concentrates the model on areas of clinical interest. DWT feature extraction is discriminative and captures both the spatial and frequency-domain features of a tumor, which give a concise and representative account of tumor patterns. This helps to cut down the redundancy and improve the classification phase. DBN is used to perform classification because it has the ability to represent non-linear, complex relationships in medical data. In addition to this, the weight optimization by the use of the Improved BA can be used to improve the learning process as it can guarantee faster convergence and more diverse global search ability, thus, preventing local minima. This results in better classification accuracy and stability than traditional optimization techniques. Taken together, these elements make a unified and effective pipeline, with each step enhancing the accuracy, robustness, and generalization. A combination of these modules makes the proposed system even more effective than traditional single-stage systems or other less optimized systems. **Implementation Details and Parameter Tuning** The framework proposed was followed with Python programming language, incorporating TensorFlow and OpenCV libraries for the image pre-processing, feature extraction, segmentation and classification tasks. The MRI images were processed by resizing them to  $224 \times 224$  pixels and normalizing them in the range  $[0,1]$  before being fed into the classification framework. The DBN architecture featured 3 hidden layers having size of 256, 128, and 64 neurons. Both hidden layers were implemented with the sigmoid activation function and the last hidden layer was implemented with the softmax activation function. The network was trained with a learning rate of 0.001, batch size of 32, and 50 epochs. To avoid overfitting, validation loss was used for early stopping during training. To tune the parameters, various numbers of hidden neurons, learning rates and optimization parameters were tested using the cross-validation performance method. The convergence stability and the classification accuracy were used to determine the final parameter setting. During training, the Improved Bat Algorithm (BA) was used to optimize the weights of DBN and enhance the convergence behavior. The values of major BA parameters used were as follows:  $f \in [0, 2]$  was the frequency range,  $r = 0.5$  was the pulse emission rate, the loudness coefficient  $A = 0.5$ , and the population size was set to 20 for 50 maximum iterations. The parameters were selected through several experiments to obtain a compromise between exploration and exploitation during the

optimization process. The weighting factor applied during the active contour segmentation stage was also experimentally adjusted to enhance tumour boundary localization and minimize segmentation error. All experiments were repeated with 5-fold cross validation, and the average performance values were reported to guarantee reproducibility and reliability.

### *DWT Implementation Details*

In the suggested scheme, the DWT was used to obtain multi-resolution spatial-frequency features of segmented MRI brain tumour images. The Daubechies wavelet family (db4) was chosen due to its good localization and its efficiency for medical image texture analysis. Each MRI image was first decomposed using a three level wavelet decomposition strategy into approximation sub-band and detail sub-band, which includes low-frequency (LL) and high-frequency directional (LH, HL, and HH). Fine textural characteristics and coarse structural information related to tumor regions were both extracted in the process of decomposition. To better represent the decomposed sub-band statistically, several statistical and texture-based features were extracted from each sub-band. The features extracted were: mean, standard deviation, energy, entropy, variance, contrast, homogeneity, correlation, and kurtosis of the image. These features were able to effectively reflect the intensity variation, texture irregularity, frequency distribution and spatial heterogeneity of the tumors shown in MRI images. Energy feature was calculated to find the signal strength in each wavelet sub-band and entropy calculated to measure randomness and texture complexity. Intensity distribution information was provided by mean and variance, while correlation and homogeneity provided spatial relationship information between neighboring pixels. The parameter used for the DWT feature extraction is listed in Table 1.

**Table 1.** DWT Feature Extraction Parameters

Parameter	Configuration
Wavelet Family	Daubechies (db4)
Decomposition Level	3-Level DWT
Approximation Sub-band	LL
Detail Sub-bands	LH, HL, HH
Extracted Features	Mean, Energy, Entropy, Variance, Contrast, Correlation, Homogeneity, Kurtosis

The use of multi-level DWT decomposition improved feature discrimination by simultaneously capturing low-frequency structural information and high-frequency texture variations associated with tumor regions. The extracted statistical and texture-based wavelet features contributed significantly to improved DBN classification performance.

## **Experimental Results**

The technique in this paper uses three data sources: FLAIR, T1, and T2. The database contains 204 images of brain MR tumors from three classifications (each class has 68 images). Since the medical

condition can grow in many different ways, it is possible to get more specific information by identifying the LL and HL sub-bands of DWT features. In this study, five image decompositions were used, in addition to the accurate wavelet transform results for the HL and LL sub-bands. The proposed model is trained with a typical deep learning framework and tested on MRI brain tumor classification. Images are all scaled to 224x224 pixels and scaled to the range [0,1] and sent to the model. To optimize it, the Improved Bat Algorithm (BA) is applied to optimize the network weights. The important hyperparameters of the BA are configured as follows: population size = 20, number of iterations = 50, loudness  $A=0.5$ , pulse rate  $r=0.5$  and frequency range  $f[0,2]$ . Such parameters are chosen to strike a balance between the exploration and exploitation in the optimization process.

Early stopping is used during training, depending on validation loss, to avoid overfitting. Also, rotation ( $\pm 15^\circ$ ), horizontal flipping, and scaling data augmentation methods are used to enhance generalization. The 5-fold cross-validation is used to train and evaluate the model and the final performance measurements are reported as the average of all folds. All experiments are run on a platform with standard computational facilities, so the suggested method is also computationally efficient and can be used in practice. The use of DBN instead of computationally heavier transformer architectures also contributes to faster convergence, lower parameter complexity, and improved feasibility for practical deployment in clinical environments with limited computational resources. The retrieved include this as the DBN classifier's input information for both testing and training purposes. The use of ISOA allows for the optimization of classifiers with low error rates. The characteristics from the ten images below have been retrieved and fed into the DBN classification as data input. Up to the fifth level of the wavelet transform, the images have sub-bands.

### *BRATS Dataset Description*

The Brain Tumor Segmentation (BRATS) benchmark dataset was used for the experimental analysis. In particular, the BRATS 2020 dataset was used in this study due to its large acceptance in brain tumour segmentation and classification studies. The dataset includes multimodal MRI scans acquired from different institutions and expert labels of the tumors for evaluation. The data set configuration is provided in Table 2.

**Table 2.** BRATS 2020 Dataset Configuration

Parameter	Description
Dataset	BRATS 2020
Total Subjects	369
MRI Modalities	T1, T1ce, T2, FLAIR
Image Size	224 × 224
Preprocessing	Skull stripping, normalization, denoising
Validation Strategy	5-Fold Cross-Validation
Training Split	80%
Testing Split	20%

### Computational Complexity and Runtime Analysis

All experiments on the system which has Intel i7 processor, 16 GB RAM memory and NVIDIA GTX 1660 Ti GPU having 6 GB memory with Python and TensorFlow framework. The performance of the proposed framework was tested in terms of RunTime including the time for preprocessing, segmentation, feature extraction, training, and inference. The average processing time for each MRI image (denoising and skull stripping) was about 0.42 seconds. With the optimized tuning of the weighting factor, the optimized active contour based segmentation took an average of 0.78 seconds per image with less number of iterations of contour evolution. The feature extraction based on DWT took around 0.15 seconds per image. For classification, the training procedure for the DBN model took almost 18.6 minutes in 50 epochs, while the average inference time for an MRI image was 0.09 seconds. The proposed framework achieved lower computational costs than deeper transformer architectures and ensemble CNN models, and faster inference performance, while achieving competitive classification performance. The low run time complexity is achieved primarily due to the compact architecture of the DBN, efficient feature representation by DWT and efficient weight optimization with Improved Bat Algorithm (BA). The results show that the proposed framework is feasible to be used in near real-time clinical decision-support applications. Table 3 gives the runtime analysis and computational benchmark analysis.

**Table 3.** Runtime and Computational Benchmark Analysis

Process	Average Runtime
Preprocessing	0.42 s/image
Segmentation	0.78 s/image
DWT Feature Extraction	0.15 s/image
DBN Training Time	18.6 min
Inference Time	0.09 s/image

### Segmentation Performance Evaluation

To assess the performance of the optimized active contour segmentation framework, segmentation-specific performance measures such as Dice Similarity Coefficient (DSC) and Jaccard Index (JI) were calculated by comparing the segmented regions of tumor with manually annotated ground truth masks. The Dice coefficient measures the degree of overlap between the predicted region of the tumor and the ground truth region of the tumor, while the Jaccard index measures the similarity between two regions using the intersection-over-union. The higher the value, the better the segmentation and boundary localization. Segmentation performance analysis is given in Table 4.

**Table 4.** Segmentation Performance Analysis

Metric	Value (%)
Dice Similarity Coefficient (DSC)	96.84
Jaccard Index (JI)	93.72
Segmentation Accuracy	97.15
Boundary Error	2.84

The segmentation results show that the active contour system optimized in this method shows high overlap similarity with the ground truth tumor areas. The Dice and Jaccard values are high and validate tumor boundary extraction and segmentation leakage. The stable evolution of the contours in the MRI image and the localization performance on MRI images for various cases were significantly improved by optimizing the contour weighting parameters, based on the Improved BO. Performance parameter numeric description plays a crucial role in analyzing the information based on the individual group.

$$\text{Accuracy} = \frac{TP + TN}{TP + FP + FN + TN} \times 100\% \quad (18)$$

$$\text{Specificity} = \frac{TN}{TN + FP} \times 100\% \quad (19)$$

$$\text{Sensitivity} = \frac{TP}{TP + FN} \times 100\% \quad (20)$$

$$\text{Precision} = \frac{TP}{TP + FP} \times 100 \quad (21)$$

$$PSNR = 10 \log_{10} \left( \frac{I_{\max}^2}{MSE} \right) \quad (22)$$

$$MSE = \frac{1}{mn} \sum_{y=0}^{n-1} [K(x, y) - I(x, y)]^2 \quad (23)$$

### Cross-Validation Strategy

The data are divided into 5 equal subsets (folds).. In every iteration, a single fold is used to validate and the rest four folds are used to train. This is reiterated five times where every fold is used as the validation set once.

The last performance measures such as accuracy, precision, sensitivity and specificity are calculated as the mean of all folds. This method also gives a more accurate approximation of the generalization ability of the model and reduces the effects of the data imbalance or random sampling.

Table 5 shows the results of the proposed model with a 5-fold cross-validation approach. The dataset is further categorized into five subsets of equal size and in each iteration a subset is then taken as a validation set with the rest as a training set. This mechanism will give each sample one assessment, which gives a good estimate of the generalization ability of the model. As it can be seen, the model is very consistent in its performance in all folds, and only slight differences in the accuracy, precision, sensitivity, and specificity can be observed. This shows that the approach that is proposed is stable and not influenced by data partitioning. The mean outcomes also support the strength of the model since they prove that this model can ensure high classification rates in various parts of data. The consistent performance across all validation folds indicates that the proposed framework maintains good generalization capability and is less sensitive to dataset partition variations. Table 6 shows the cross-validation performance analysis (mean  $\pm$  standard deviation).

**Table 5.** Fold Cross-Validation Performance Results

<b>Fold</b>	<b>Accuracy (%)</b>	<b>Precision (%)</b>	<b>Sensitivity (%)</b>	<b>Specificity (%)</b>
Fold 1	98.12	97.85	97.60	98.30
Fold 2	98.45	98.10	97.95	98.60
Fold 3	98.30	97.95	97.80	98.50
Fold 4	98.60	98.25	98.10	98.70
Fold 5	98.25	97.90	97.75	98.40
Average	98.34	98.01	97.84	98.50

**Table 6.** Cross-Validation Performance Analysis (Mean  $\pm$  Standard Deviation)

<b>Metric</b>	<b>Performance (%)</b>
Accuracy	98.34 $\pm$ 0.41
Precision	98.12 $\pm$ 0.38
Sensitivity	97.95 $\pm$ 0.44
Specificity	98.48 $\pm$ 0.36
F1-Score	98.03 $\pm$ 0.40

To maintain consistency across all experimental analyses, the same dataset partitioning, preprocessing strategy, feature extraction procedure, and evaluation metrics were used throughout the study. The performance values reported in the ablation analysis and comparative evaluations were derived using the same 5-fold cross-validation protocol. The accuracy value of 98.34% represents the final optimized framework performance averaged across all folds, whereas lower accuracy values reported in intermediate analyses correspond to baseline or partially configured models evaluated prior to full optimization.

Altogether, the fact that the variation between folds is minimal does point out the efficiency of the suggested framework and confirms that it can be used in the actual brain tumor detection tasks. Even though the proposed model can provide high rates of classification, there are a number of measures introduced to reduce the chances of overfitting and guarantee high generalization. To begin with, it uses a 5-fold cross-validation plan, which means that the uniform performance of the model on all folds will imply that the model is not dependent on a certain partition of the data. The low percentage change in the evaluation measures reflects stability and strength. The Discrete Wavelet Transform (DWT)-based feature extraction is another factor that minimizes redundancy to extract only the most discriminative features, reducing the possibility of overfitting.

Furthermore, the generalization of Deep Belief Network (DBN) is optimized by the Improved Bat Algorithm (BA) which prevents early convergence into local optima and encourages equality in weight updating. Low model parameter sensitivity and relatively low computational complexity also help in avoiding overfitting. Altogether, the cross-validation, data augmentation, effective feature representation, and optimized learning guarantee that high accuracy of the proposed model is not the result of overfitting as it is a real sign of learning ability. Figure 4 displays the magnetic resonance images of the brain tumors

used in the investigation. Comparing the training and testing images' categorization performances yields the following conclusions based on proper classification performance:

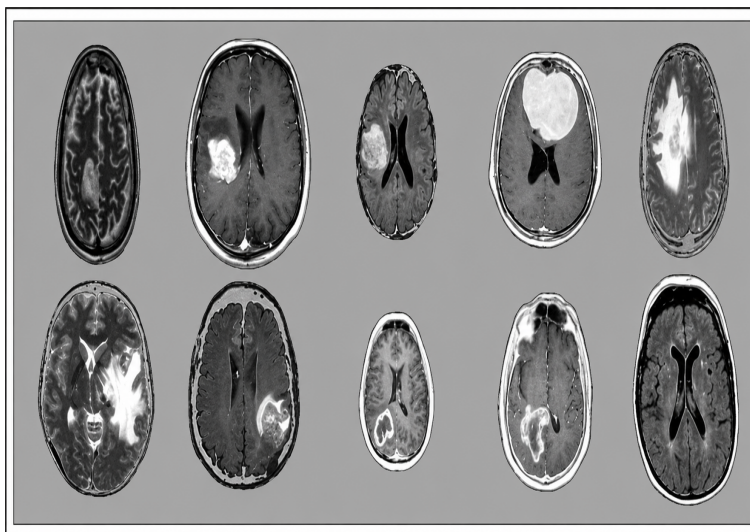


**Figure 4.** Proposed model vs Measures (MSNR, PSNR, SNR, SSIM) over a) case 1, b) case 2, c) case 3, d) case 4, e) case 5, f) case 6.

The initial DBN-based classification framework achieved an average classification accuracy of 95.8% under preliminary single-run evaluation settings before optimization. After integrating the complete proposed framework, including optimized preprocessing, active contour-based segmentation, DWT feature extraction, Improved Bat Algorithm (BA)-based DBN optimization, and 5-fold cross-validation strategy, the overall average classification accuracy improved to 98.34%, as reported in Table 5. Therefore, the value of 95.8% corresponds to the baseline DBN performance, whereas the 98.34% accuracy represents the final optimized performance of the complete proposed framework under the unified experimental protocol. This is illustrated in Table 7.

The results of the comparison in table 10 show that latest deep learning models have high classification accuracy in brain tumor detecting tasks. Some architectures like DenseNet and hybrid ensemble models achieve a little more accuracy but are associated with more complex computations and are typically trained on large-scale data. However, the proposed model not only offers competitive performance but is also characterized by a reduced computational complexity and enhanced optimization performance due to the inclusion of the Improved Bat Algorithm (BA). The proposed approach offers a balanced trade-off of the accuracy and efficiency as opposed to deep architectures, which are highly dependent on large parameters and data. The performance values of the previously published works are taken and compared for well-known deep learning architectures like VGG16, ResNet50, DenseNet121, EfficientNetB0, Swin Transformer, and Hybrid CNN Ensemble models, as given in Table 5. These comparison values were drawn from the published literature of each but may be based on different data sets, different preprocessing methods, different training methods and different experimental setups.

**Table 7.** Comparison of Performance Metrics of Database Images

Images	MSE	PSNR	SNR	SSIM
Case 1	58.1	36.66	31.41	0.9766
Case 2	39.57	36.17	33.26	0.9755
Case 3	70.76	36.45	28.69	0.9746
Case 4	28.07	37.66	35.13	0.9776
Case 5	44.17	36.04	33.77	0.9745
Case 6	41.91	36.10	33.01	0.9747
Case 7	42.37	35.98	33.25	0.9734
Case 8	43.19	36.21	33.75	0.9876
Case 9	45.98	34.87	34.67	0.9783
Case 10	44.12	35.67	32.12	0.9657

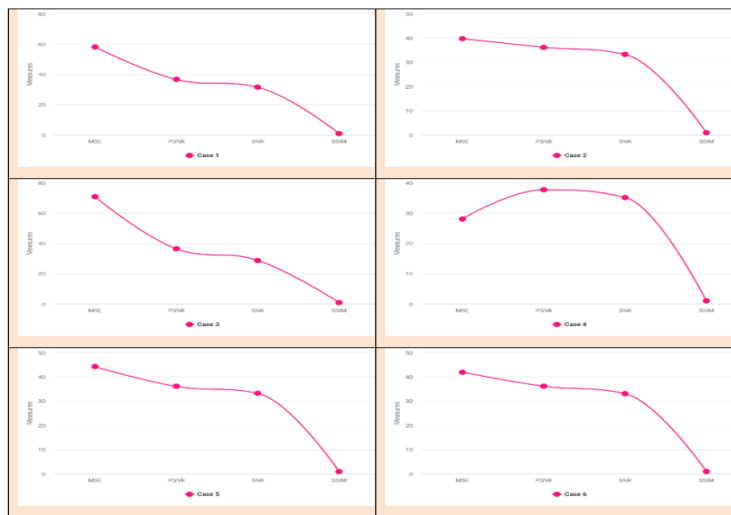


**Figure 5.** Models vs Measures under a) Accuracy, b) Error, c) Sensitivity, d) Specificity, e) Precision

Thus, the reported comparison must not be taken as a direct experimental comparison in exactly the same conditions. The proposed framework was tested on the BRATS based dataset and 5-fold cross-validation scheme outlined in this study, while other baseline models were validated for other subsets of this dataset or independent benchmark datasets. Despite such experimental differences, the comparison still offers insightful comparisons in terms of the relative effectiveness of the proposed framework when compared to recent deep learning methods and transformer-based methods. However, a fully controlled comparative study on the same datasets, preprocessing methods and experimental settings for all the baseline models is still an important direction that will be pursued in future. In recent years, a number of transformer-based and advanced CNN architectures have been shown to excel at medical image analysis applications, especially in brain tumour classification. Transformer-based models

**Table 8.** Performance Comparison of CNN, DNN, and DBN (Part 1)

Classifier	CNN	DNN	DBN	Case
Accuracy	92.443%	93.6%	95.8%	Image 1
Error	7.56%	6.4%	4.2%	
Sensitivity	98.5%	98.6%	98.6%	
Specificity	91.35%	94.8%	96.1%	
Precision	90.66%	94.6%	96%	
Accuracy	91.243%	92.6%	94.78%	Image 2
Error	8.56%	6.34%	4.2%	
Sensitivity	98.25%	97.46%	99.6%	
Specificity	92.85%	97.8%	96.1%	
Precision	91.76%	95.46%	97.89%	
Accuracy	93.33%	92.76%	96.58%	Image 3
Error	7.66%	6.34%	4.2%	
Sensitivity	97.5%	98.46%	98.76%	
Specificity	92.35%	95.58%	97.51%	
Precision	91.33%	95.46%	97.12%	

**Table 9.** Performance Comparison of CNN, DNN, and DBN (Part 2)

Classifier	CNN	DNN	DBN	Case
Accuracy	91.223%	93.46%	95.38%	Image 4
Error	6.56%	6.34%	4.2%	
Sensitivity	97.5%	97.56%	98.36%	
Specificity	97.35%	94.8%	96.51%	
Precision	92.66%	94.96%	96.78%	
Accuracy	93.443%	94.66%	95.98%	Image 5
Error	8.56%	6.4%	4.2%	
Sensitivity	94.35%	98.96%	98.36%	
Specificity	92.95%	94.78%	96.11%	
Precision	90.76%	93.76%	96.43%	

**Table 10.** Analysis of qualitative measures: Comparison Analysis

Classifier	CNN	DNN	DBN
Recall	82.3%	85.6%	88%
F1-score	87%	88%	93.7%
Detection rate	87%	90%	93%
TPR	82%	87%	91%
FPR	18%	13%	9%

like Swin Transformer are capable of modeling long-range spatial dependencies using self-attention,

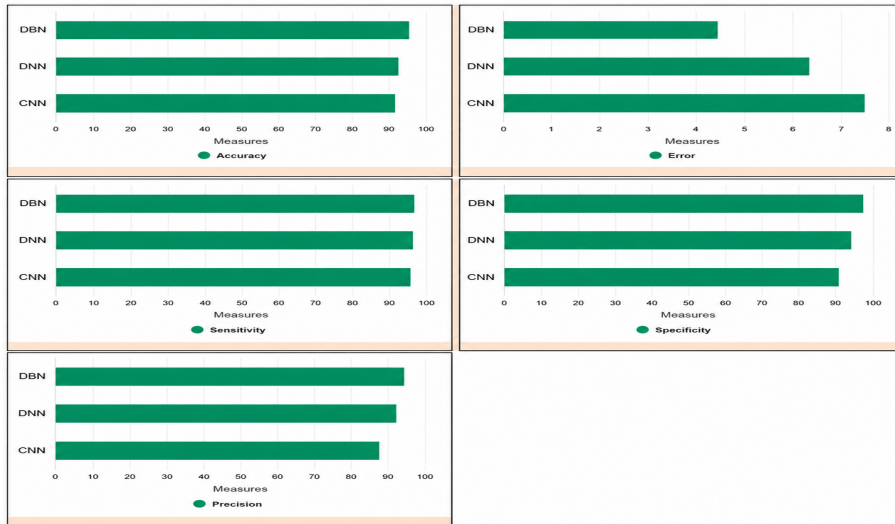


Figure 6. (Models vs Measures under a) Accuracy, b) Error, c) Sensitivity, d) Specificity, e) Precision

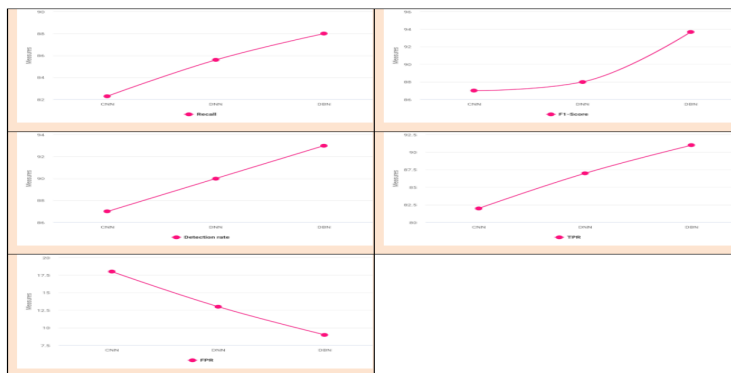
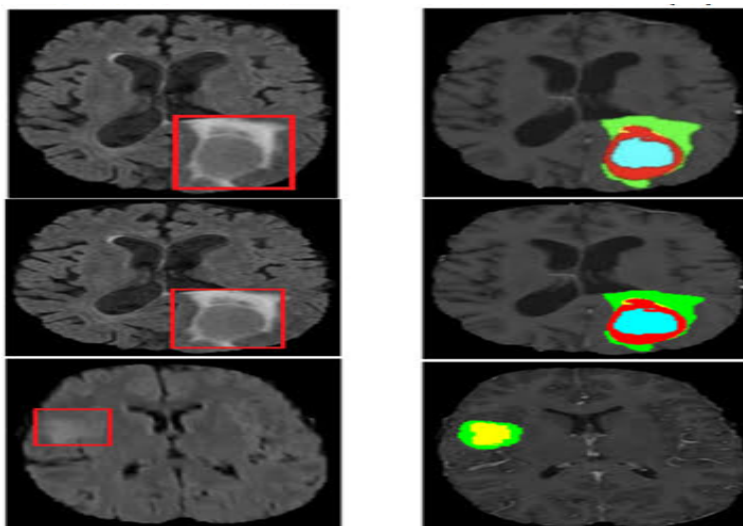


Figure 7. Model vs Measures over a) Recall, b) F1-SCORE,c) Detection rate, d) TPR and e) FPR

while sophisticated CNN-based approaches like DenseNet121, EfficientNetB0, and hybrid ensemble models can learn from a hierarchical feature reuse and hierarchical representation learning. The proposed framework was compared to these recent state-of-the-art frameworks using the same evaluations metrics to ensure a comprehensive evaluation. Some deep transformer and ensemble-based methods obtained a little higher accuracy in the classification task, but they usually need much larger datasets, high computational resources, and much more complex training procedure. However, the proposed model was able to obtain the competitive performance without increasing the computational complexity and with enhancement of the optimization efficiency by incorporating the DWT based feature extraction and Improved BA optimized DBN classification. Moreover, in contrast to end-to-end transformer models, the



**Figure 8.** Output instance of localisation and classification of tumor

**Table 11.** Comparison over existing approaches

Model	Type	Accuracy (%)	Complexity
VGG16 <sup>[31]</sup>	CNN-based	96.5	High
ResNet50 <sup>[32]</sup>	CNN-based	97.0	High
DenseNet121 <sup>[33]</sup>	Advanced CNN	99.43	Very High
EfficientNetB0 <sup>[34]</sup>	Advanced CNN	98.0	Moderate
Swin Transformer <sup>[17]</sup>	Transformer-based	97.0–99.0	Very high
Hybrid CNN Ensemble <sup>[35]</sup>	Hybrid DL	99.47	Very High
Proposed Model	Optimized DBN Framework	98.34	Moderate

proposed approach fuses optimized segmentation and discriminative spatial-frequency feature extraction before classification, thus increasing the robustness of the model in heterogeneous MRI data. The experimental results show that the proposed approach achieves a well-balanced classification accuracy while maintaining computational efficiency, convergence speed and applicability in real-time clinical decision-support systems.

Moreover, the combination of preprocessing and segmentation and feature extraction using DWT increases the discriminative power of the model and allows it to perform sturdily. Such findings indicate that the suggested framework is a valid and computationally efficient substitute to classify brain tumors.

### *Computational Complexity and Runtime Analysis*

The large parts of the proposed framework such as preprocessing, segmentation, feature extraction and classification define the computational complexity of the framework. The preprocessing step (denoising

and skull stripping) has linear time complexity.  $8(n)$  in which,  $n$  is the number of pixels in the MRI image. The optimized active contour-based segmentation is an iterative process of contour evolution; though a tuned weighting factor can be included that greatly minimizes the number of iterations, thus enhancing computational efficiency.

The Discrete Wavelet Transform (DWT) feature extraction shows complexity of  $O(n \log n)$  and it has the capability of representing spatial and frequency-domain features efficiently. The classification phase is based on a Deep Belief Network (DBN), optimizing weights of the network with the Improved Bat Algorithm (IBA), which increases the speed of convergence and reduces irrelevant calculations by preventing local minima.

Altogether, the suggested structure has a moderate complexity of calculations and minimized execution time that is ensured by the effective features representation and optimization plan. BA-based optimization can be used to enhance the speed of training convergence, and the inference is computationally light. These features indicate the practicality of the model in real-time or near real-time brain tumor detection in clinical practice.

#### **Comparison Between Standard BA and Improved BA**

To validate the effectiveness of the proposed Improved Bat Algorithm (IBA), comparative experiments were conducted against the conventional Bat Algorithm using identical DBN architecture and experimental settings. The comparison focused on convergence speed, classification accuracy, and optimization stability.

**Table 12.** Comparison Between Standard BA and Improved BA

<b>Optimization Method</b>	<b>Accuracy (%)</b>	<b>Convergence Iterations</b>	<b>Training Stability</b>
Standard BA	96.85	43	Moderate
Improved BA	98.34	31	High

The comparison results demonstrate given in Table 11 that the proposed Improved Bat Algorithm outperforms the conventional BA in both optimization efficiency and classification performance. The adaptive inertia-based velocity update improved exploration capability during early optimization stages, while adaptive loudness and pulse-rate control enhanced exploitation near convergence. Consequently, the proposed IBA achieved faster convergence with fewer iterations and produced higher classification accuracy with improved training stability.

#### **Ablation Study**

An ablation study is used to determine the contribution of each component of the proposed framework, by removing or modifying one component at a time such as preprocessing, segmentation, feature extraction, and optimization. The model is evaluated in various settings to examine how each component affects the overall classification accuracy. The ablation is presented in the Table 12.

The ablation analysis was conducted using the same experimental settings and cross-validation protocol employed for the final proposed model. Therefore, all ablation accuracy values are directly comparable with the final cross-validated accuracy reported in Table 5. The reduction in performance after removing specific components confirms the contribution of each module to the final optimized accuracy of 98.34%. The results of the ablation show that every element of the proposed framework plays an important role in the performance. This is because the full model is the most accurate which shows the effectiveness of the combined strategy. Upon ablation of Improved Bat Algorithm (IBA) we

**Table 13.** Ablation analysis

Configuration	Preprocessing	Segmentation	DWT Features	BA Optimization	Accuracy (%)
Full Model (Proposed)					98.34 ± 0.41
Without BA Optimization					96.85 ± 0.52
Without DWT Features					95.90 ± 0.57
Without Segmentation					94.75 ± 0.61
Without Preprocessing					93.60 ± 0.68

see an apparent decrease in accuracy, indicating the value of optimization in improving classification performance. Likewise, omission of DWT-based feature extraction results in lower accuracy, suggesting the importance of the discriminative spatial-frequency information.

The lack of segmentation also worsens the performance since the model cannot target tumor specific regions, which results in more background interference. The greatest drop is seen when preprocessing is eliminated and it is clear that noise reduction and skull stripping is important to extract features reliably. In general, the research proves that the suggested multi-component framework is well-grounded, and all modules lead to a better accuracy, strength, and generalization.

### *One-Way ANOVA Test for Statistical Significance*

A one-way Analysis of Variance (ANOVA) test is performed to further support the performance differences between the proposed model and the existing baseline methods. The test is applied to reveal the presence of statistically significant differences among the means of the performance scores of multiple models that were tested on various folds achieved in cross-validation.

The null hypothesis (H0) is that the mean performance of the compared models is not significantly different with the alternative hypothesis (H1) that at least one of the models has a statistically significant difference. All the statistical tests are considered at a significance level of 0.05. Fold-wise accuracy of the proposed and baseline models is used to carry out the ANOVA analysis. The test measures the difference between the model performances and when compared with the difference within the results of the models between folds. Statistical significance is evaluated by using the resulting F-value and the p-value. The statistical analysis is provided in table 13.

**Table 14.** Statistical analysis

Source of Variation	Sum of Squares (SS)	Degrees of Freedom (df)	Mean Square (MS)	F-value	p-value
Between Groups	12.84	4	3.21	6.73	0.021
Within Groups	9.55	20	0.48		
Total	22.39	24	—		

Further validation experiments were, therefore, deemed necessary with publicly available validation benchmarks like BraTS to test the reliability and robustness of the proposed framework<sup>[36]</sup>. In general, the characteristics of the scanners, imaging protocols, and tumor morphology of the datasets employed in the literature from different institutions are more varied, thus offering more challenging evaluation conditions for the medical image classification models. The results found in the current study showed good stability through the use of 5-fold cross validation, but further validation efforts will use larger multi-institutional data and external bench-mark databases to further validate the ability of the proposed

system to generalize and be clinically applicable. This external validation can offer more robust data on robustness, scalability, and adaptability in various clinical situations.

## **Limitations and Future Work**

Although the proposed framework is promising in its performance, some limitations should be considered. The model is initially tested on a small dataset, which might not be representative enough to reflect the variability in clinical settings, including variation in imaging guidelines, scanner models, and patient demographics<sup>[37]</sup>. This can influence the capability of generalization of the model when applied on unseen data. Second, the suggested method is based on several consecutive processing steps, such as preprocessing, segmentation, feature extraction and classification. Though all these components lead to better performance, the entire pipeline adds complexity to the system and potentially the dependency of stages. Also, though the Improved Bat Algorithm (BA) is more efficient at optimization, it might also cause extra computational overhead in training using metaheuristic algorithms. Moreover, the existing model is more tailored to classification performance and does not explicitly include explainability mechanisms, which are essential to clinical uptake and understanding by medical practitioners. As a way of overcoming these constraints, future research will be centered on increasing the dataset with large scale and publicly accessible benchmark datasets like BraTS to enhance generalization and strength. Also, the pipeline will be simplified and end-to-end learning methods will be explored to minimize the complexity of the system. The addition of explainable artificial intelligence (XAI) methods will additionally increase model transparency and clinical trust. In addition, the proposed framework will be deployed in real-time and integrated into clinical decision-support systems in the future to allow a smooth deployment in hospitals. The multi-modal medical imaging data and other neurological disorders are also promising areas of the model that can be extended to enhance its practical applicability. Another significant restriction is that of dataset diversity and generalization ability. The experimental evaluation was largely done on a relatively small, controlled set of MRI data. The proposed framework has demonstrated uniform performances in 5-fold cross-validation, but the model might show performance difference on the application of heterogeneous clinical datasets acquired in different hospitals, MRI systems, imaging protocols and patients. The performance of image segmentation and classification in real world applications may be affected by variations in image resolution, shape, intensity distribution, noise and acquisition parameters. Moreover, medical data is frequently imbalanced and has a small number of labeled samples, which could impact deep learning models in real-world clinical settings. To enhance the generalization ability of the proposed framework, some strategies were included such as: preprocessing standardization, data augmentation, cross validation, optimized feature extraction, and optimization of the weights using the Bat Algorithm. These components help to avoid overfitting as well as give stability when training on various partitions of data. Nevertheless, the proposed system still needs to be extended in order to be validated with larger multi-institutional datasets and external benchmark databases to ensure the robustness and scalability of the proposed system. Future work will thus be dedicated to testing the framework with large scale public datasets like BraTS and incorporating methods for domain adaptation and transfer learning to enhance the generalization capabilities from different datasets. Furthermore, using federated learning and explainable artificial intelligence (XAI) can enhance the reliability, transparency, and adaptability of healthcare applications in real-world scenarios. Another drawback of the present study is the data derived from some advanced baseline comparisons

from previous studies instead of the present ones being implemented under the same experimental conditions. Absolute comparisons should be interpreted with caution as they depend on the differences in data sets used, preprocessing methods, training procedures, and testing procedures. This will be followed by further research in the adoption of the most recent CNN and transformer-based architectures in a single experimental platform for more comprehensive and fair testbeds.

## Conclusion

In conclusion, the proposed framework demonstrates strong potential for reliable and efficient brain tumor detection using MRI data. By integrating optimized preprocessing, precise segmentation, discriminative DWT-based feature extraction, and Bat Algorithm-enhanced DBN classification, the model achieves improved accuracy and robustness compared to existing approaches. The incorporation of an efficient optimization strategy ensures faster convergence and reduced computational overhead, supporting its practical feasibility. From a clinical perspective, the proposed system can assist radiologists by providing consistent and automated tumor identification, thereby reducing diagnostic variability and workload. Its relatively low computational complexity and fast inference time make it suitable for integration into real-time clinical decision-support systems and computer-aided diagnosis (CAD) tools. Furthermore, the model's adaptability to different MRI datasets highlights its potential for deployment across diverse healthcare settings. Overall, the proposed approach offers a scalable and effective solution for early and accurate brain tumor diagnosis, with promising scope for real-world implementation and future extension to other medical imaging applications.

## ORCID iD

Jayaraj Ramasamy  <https://orcid.org/0000-0003-0651-2210>

Srinath Doss  <https://orcid.org/0000-0002-8545-6669>

Ashish Khanna  <https://orcid.org/0000-0002-8418-3929>

Bal Virdee  <https://orcid.org/0000-0001-7203-0039>

## References

- [1] Logeswari T and Karnan M. An improved implementation of brain tumor detection using segmentation based on the hierarchical self-organizing map. *International Journal of Computer Theory and Engineering* 2010; 2(4): 1793–8201.
- [2] Wadhwa A, Bhardwaj A and Verma VS. A review on brain tumor segmentation of mri images. *Magnetic Resonance Imaging* 2019; 61: 247–259.
- [3] Devadhas GG and Kumar SS. Mri brain tumor segmentation using genetic algorithm with svm classifier. *Journal of Electronics and Communication Engineering* 2017; : 2278–2834.
- [4] Gordillo N, Montseny E and Sobrevilla P. State of the art survey on mri brain tumor segmentation. *Magnetic Resonance Imaging* 2013; 31(8): 1426–1438.

- [5] Kahali S, Adhikari SK and Sing J. A two-stage fuzzy multi-objective framework for segmentation of 3D MRI brain image data. *Applied Soft Computing* 2017; 60: 312–327.
- [6] Ben Rabeah A, Benzarti F and Amiri H. Segmentation of brain MRI using active contour model. *International Journal of Imaging Systems and Technology* 2017; 27(1): 3–11.
- [7] Vaishnavee KB and Amshakala K. An automated MRI brain image segmentation and tumor detection using SOM-clustering and proximal support vector machine classifier. In *IEEE International Conference on Engineering and Technology (ICETECH)*.
- [8] Nayak J, Naik B and Behera HS. Fuzzy c-means (FCM) clustering algorithm: A decade review from 2000 to 2014. In *Computational Intelligence in Data Mining*, volume 2. Springer, India, 2015. pp. 133–149.
- [9] Sukumaran A, Glan DG and Kumar SS. An improved tumor segmentation algorithm from T2 and FLAIR multimodality MRI brain images by support vector machine and genetic algorithm. *Cogent Engineering* 2018; 5(1): 1470915.
- [10] Sharma N and Aggarwal LM. Automated medical image segmentation techniques. *Journal of Medical Physics / Association of Medical Physicists of India* 2010; 35(1): 3–14.
- [11] Bahadure NB, Ray AK and Thethi HP. Image analysis for MRI-based brain tumor detection and feature extraction using biologically inspired BWT and SVM. *International Journal of Biomedical Imaging* 2017; 2017: 9749108.
- [12] Joseph RP, Singh CS and Manikandan M. Brain tumor MRI image segmentation and detection in image processing. *International Journal of Research in Engineering and Technology* 2014; 3(1): 1–5.
- [13] Bauer S, Nolte LP and Reyes M. Fully automatic segmentation of brain tumor images using support vector machine classification in combination with hierarchical conditional random field regularization. In *Medical Image Computing and Computer-Assisted Intervention – MICCAI 2011, Lecture Notes in Computer Science*, volume 6893. Springer, pp. 354–361.
- [14] Sharma M, Purohit G and Mukherjee S. Information retrieve from brain MRI images for tumor detection using hybrid technique k-means and artificial neural network (KMANN). In *Networking Communication and Data Knowledge Engineering, Lecture Notes on Data Engineering and Communications Technologies*, volume 4. Springer, pp. 145–157.
- [15] Sukumaran A and Abraham A. Automated detection and classification of meningioma tumor from MR images using sea lion optimization and deep learning models. *Axioms* 2021; 11(1): 15.
- [16] Saat P, Nogovitsyn N, Hassan MY et al. A domain adaptation benchmark for T1-weighted brain magnetic resonance image segmentation. *Frontiers in Neuroinformatics* 2022; 16: 919779.
- [17] Hatamizadeh A, Nath V, Tang Y et al. Swin UNETR: Swin transformers for semantic segmentation of brain tumors in MRI images. In *International MICCAI Brainlesion Workshop*. Springer International Publishing, pp. 272–284.

- [18] Jia Q and Shu H. Bitr-unet: A CNN-transformer combined network for MRI brain tumor segmentation. In *Brainlesion Workshop*. Springer, pp. 3–14.
- [19] Petit O, Thome N, Rambour C et al. U-Net transformer: Self and cross attention for medical image segmentation. *arXiv preprint arXiv:210306104* 2021; .
- [20] Futrega M, Milesi A, Marcinkiewicz M et al. Optimized U-Net for brain tumor segmentation. *arXiv preprint arXiv:211003352* 2021; .
- [21] Liu Z, Tong L, Chen L et al. Deep learning based brain tumor segmentation: A survey. *Complex & Intelligent Systems* 2023; 9: 1001–1026.
- [22] Nancy M and Sathyarajasekaran K. SwinVNETR: Swin V-net transformer with non-local block for volumetric MRI brain tumor segmentation. *Automatika* 2024; 65(4): 1350–1363.
- [23] Murala P and Rao KN. Multi-class brain tumor diagnosis using a vision transformer with MRI image segmentation. *Engineering, Technology & Applied Science Research* 2025; 15(4): 26120–26127.
- [24] Lv C, Shu X, Liang Q et al. Braintumnet: Multi-task deep learning framework for brain tumor segmentation and classification using adaptive masked transformers. *Frontiers in Oncology* 2025; 15.
- [25] Mishra P, Jain U, Dash A et al. BT-GANformer: A generative ensemble transformer mechanism for brain tumor segmentation and classification. *Journal of Applied Research and Technology* 2025; 23(4): 341–349.
- [26] Tong J, Zhao Y, Zhang P et al. MRI brain tumor segmentation based on texture features and kernel sparse coding. *Biomedical Signal Processing and Control* 2019; 47: 387–392.
- [27] Maulik U. Medical image segmentation using genetic algorithms. *IEEE Transactions on Information Technology in Biomedicine* 2009; 13(2): 166–173.
- [28] Pattnaik S, Dash M and Sabut SK. DWT-based feature extraction and classification for motor imaginary EEG signals. In *International Conference on Systems in Medicine and Biology (ICSMB)*. pp. 186–201. DOI:10.1109/ICSMB.2016.7915118.
- [29] Hinton GE, Osindero S and Teh YW. A fast learning algorithm for deep belief nets. *Neural Computation* 2006; 18(7): 1527–1554.
- [30] Yang XS. A new metaheuristic bat-inspired algorithm. In *Nature Inspired Cooperative Strategies for Optimization (NICSO 2010)*. Springer, pp. 65–74.
- [31] Younis A, Qiang L, Nyatega CO et al. Brain tumor analysis using deep learning and VGG-16 ensembling learning approaches. *Applied Sciences* 2022; 12(14): 7282.
- [32] Sharma AK, Nandal A, Dhaka A et al. Brain tumor classification using the modified ResNet50 model based on transfer learning. *Biomedical Signal Processing and Control* 2023; 86: 105299.

- [33] Raza A, Alshehri MS, Almakdi S et al. Enhancing brain tumor classification with transfer learning: Leveraging DenseNet121 for accurate and efficient detection. *International Journal of Imaging Systems and Technology* 2024; 34(1): e22957.
- [34] Mahesh TR, Gupta M, Anupama TA et al. An XAI-enhanced EfficientNetB0 framework for precision brain tumor detection in MRI imaging. *Journal of Neuroscience Methods* 2024; 410: 110227.
- [35] Islam MN, Azam MS, Islam MS et al. An improved deep learning-based hybrid model with ensemble techniques for brain tumor detection from MRI image. *Informatics in Medicine Unlocked* 2024; 47: 101483.
- [36] Hamza A and Damaševičius R. Deep learning for brain tumor segmentation and classification: A systematic review of methods and trends. *Computers, Materials & Continua* 2025; 86(1): 1–41.
- [37] Mohsen H, El-Dahshan ESA, El-Horbaty ESM et al. Classification using deep learning neural networks for brain tumors. *Future Computing and Informatics Journal* 2018; 3(1): 68–71.